



Article

# Theoretical Investigation of Vibrational Frequencies and Electronic Structure Properties of Tetrathiafulvalene (TTF) Using Density Functional Theory (DFT) with DMol<sup>3</sup> Quantum Software

Aya Adnan Ibrahim<sup>1</sup>, Abdulhakim Sh. Mohammed<sup>2</sup>

1,2. Department of Physics, college of Education for pure sciences, University of Kirkuk, Iraq

**Abstract:** This study aims to conduct a comprehensive theoretical analysis of the structural, electronic and vibrational properties of the organic compound tetrathiafulvalene (TTF), based on Density Functional Theory (DFT) and employing the Dmol<sup>3</sup> quantum computational program. Three different exchange–correlation functionals—LDA-PWC, GGA-PBE, and the hybrid B3LYP—were utilized to compare their performance in describing the molecular characteristics of TTF. Geometry optimization revealed noticeable variations in bond lengths and angles depending on the chosen functional, with B3LYP demonstrating the closest agreement with reference experimental data. The analysis of the frontier molecular orbitals (HOMO and LUMO) showed significant differences in the energy gap, where B3LYP again proved to be more accurate in predicting electronic stability and chemical reactivity. Global chemical reactivity descriptors—such as ionization potential, electron affinity, chemical hardness and softness, electronegativity, and electrophilicity index—were also calculated, and the results using B3LYP showed strong consistency with previously reported theoretical values. Furthermore, the vibrational spectrum of TTF was computationally examined and categorized into three regions: a low-frequency region (0–1000 cm<sup>-1</sup>) corresponding to sulfur atom bending and C–S bond modes; a mid-frequency region (1000–1600 cm<sup>-1</sup>) involving C=C stretching and C–H bending vibrations; and a high-frequency region (1600–3200 cm<sup>-1</sup>) associated with high-energy C–H stretching. Slight differences in peak positions and intensities were observed among the functionals, attributed to variations in the treatment of electron exchange and correlation. Overall, the study underscores the importance of functional selection in theoretical modeling and offers valuable insights into the behavior of the TTF molecule, reinforcing its potential for applications in organic electronics and advanced materials.

**Citation:** Ibrahim, A. A., Mohamaed, A. S. Theoretical Investigation of Vibrational Frequencies and Electronic Structure Properties of Tetrathiafulvalene (TTF) Using Density Functional Theory (DFT) with DMol<sup>3</sup> Quantum Software. Central Asian Journal of Medical and Natural Science 2025, 6(4), 1438-1453.

**Keywords:** TTF, DFT, FMOs, GCRDS, Infrared Spectroscopy

Received: 31<sup>st</sup> May 2025

Revised: 9<sup>th</sup> Jun 2025

Accepted: 23<sup>rd</sup> Jun 2025

Published: 4<sup>th</sup> Jul 2025



**Copyright:** © 2025 by the authors. Submitted for open access publication under the terms and conditions of the Creative Commons Attribution (CC BY) license (<https://creativecommons.org/licenses/by/4.0/>)

## 1. Introduction

Tetrathiafulvalene (TTF) is a sulfur-rich heterocyclic compound with the molecular formula C<sub>6</sub>H<sub>4</sub>S<sub>4</sub> and a molecular weight of 204.4 g/mol [1]. This compound has played a pivotal role in the advancement of organic electronics and materials science due to its unique chemical and physical properties [2].

TTF is a planar organic molecule featuring a  $\pi$ -conjugated system, consisting of two thiolate rings connected by a central double bond. In its neutral form, TTF is electrically neutral and exhibits poor conductivity. However, it readily undergoes oxidation to form

radical cations such as  $\text{TTF}^{+\bullet}$  and  $\text{TTF}^{2+}$ , which are instrumental in facilitating charge transport [3].

The discovery of TTF dates back nearly a century, with its derivatives first identified as by-products in organic reactions during the early 20th century. In 1926, a dibenzo-TTF derivative was synthesized, but the parent compound TTF remained relatively obscure until the early 1970s, when Wudl and colleagues successfully synthesized it and elucidated its unusual redox and electrical conductivity properties [4].

Structurally, TTF consists of two 1,3-dithiol rings linked by a central double bond, forming a planar system composed of two fused rings, as illustrated in Figure (1).

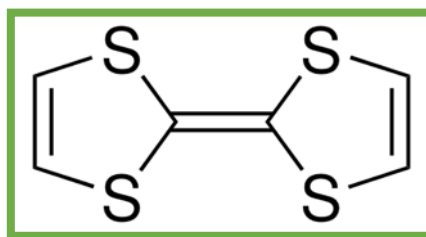


**Figure 1.** The chemical structure of the TTF molecule.

Tetrathiafulvalene (TTF) is considered one of the key conductive organic molecules, though it is not a traditional semiconductor on its own. Its significance lies in its role as a fundamental component in the development of organic semiconductors through the formation of charge-transfer complexes and molecular conductors. To understand this in depth, it is essential to analyze its electronic behavior in both its neutral and oxidized states [5].

The molecule's distinctive properties—such as thermal stability, redox activity, and planar structure—make TTF a central building block in the design of organic electronic devices, including organic transistors, photovoltaic solar cells, and radical cation-based organic semiconducting materials [6].

This study primarily relies on quantum mechanical calculations, particularly Density Functional Theory (DFT), to analyze the structural and electronic behavior of the TTF molecule, emphasizing the accuracy of computational modeling and its ability to replicate experimental reality. Three different exchange–correlation functionals within the DFT framework were employed: the Local Density Approximation (LDA), the Generalized Gradient Approximation (GGA), and the hybrid functional B3LYP. These were utilized to optimize the molecular geometry and assess the influence of each functional on the structural and electronic outcomes.

The research begins by analyzing the optimized molecular geometry, a crucial step that directly impacts vibrational modes and electronic properties. The stability of the computed geometry was validated through vibrational frequency analysis to ensure the absence of imaginary frequencies.

The application of DFT to molecular chemical systems has garnered significant attention due to its computational efficiency compared to traditional quantum mechanical bonding methods [7]. Theoretical computational methods, such as geometry optimization, are of great importance in understanding and predicting pathways of electron and energy transfer in photoactive molecular assemblies [8].

Accordingly, a set of properties were investigated, including electronic characteristics through the analysis of frontier molecular orbitals (HOMO and LUMO) and the calculation of the energy gap. It was observed that differences among the functionals had a significant effect on the estimated values of ionization potential, electron affinity, vibrational spectra, and the electronic structure of the TTF molecule in the infrared region. These analyses were

conducted using DFT with the LDA, GGA, and B3LYP functionals as implemented in the Dmol<sup>3</sup> quantum program.

This research aims to place its findings in the context of previous studies, offering a critical analysis of any potential inconsistencies and explaining their origins—whether methodological or due to the limitations of computational approaches. In doing so, the study provides deep insights into the fundamental properties of the TTF molecule and underscores its relevance in guiding future research in organic electronics and advanced materials science.

## 2. Materials and Methods

In this study, the structural, electronic, and vibrational properties of the tetrathiafulvalene (TTF) molecule were investigated using a series of Density Functional Theory (DFT) calculations implemented via the Dmol<sup>3</sup> software package [9]. Three comparative exchange–correlation functionals were employed to provide a detailed analysis of the molecule's characteristics: LDA-PWC, GGA-PBE, and the hybrid functional B3LYP. For each functional, geometry optimization was performed under nearly identical numerical conditions, with slight variations in symmetry settings and functional-specific parameters to better capture the electronic structure of TTF.

Geometry optimizations across all three methods were conducted using strict convergence criteria: an energy convergence threshold of  $1.0 \times 10^{-5}$  atomic units, a gradient convergence of  $2.0 \times 10^{-3}$  Å, and a displacement convergence of  $5.0 \times 10^{-3}$  Å. A maximum of 50 optimization cycles was allowed, with a maximum per-cycle displacement capped at 0.3000 Å. An improved initial Hessian matrix was used to accelerate convergence. The self-consistent field (SCF) procedure was configured with a density convergence threshold of  $1.0 \times 10^{-6}$ , a charge mixing parameter of 0.200, six Pulay DIIS iterations, and a maximum of 50 SCF cycles per step. Density fitting was applied up to the hexadecapole level, with a fine integration grid and a global Fermi smearing of 4.0000 Å uniformly used across all calculations.

For LDA-PWC calculations, electronic parameters were defined using spin-unrestricted polarization and a net neutral charge. A double numerical basis set with polarization functions (dnp) was selected, without employing pseudopotentials, and the exchange–correlation functional “pwc” was used. Molecular symmetry was activated in this setup to exploit the inherent symmetry of TTF, thereby reducing computational cost and enhancing stability.

Within the GGA-PBE framework, the same task parameters and convergence criteria were maintained, with the only change being the substitution of the LDA functional with “pbe,” which incorporates gradient corrections to the electron density. As with LDA-PWC, spin-unrestricted polarization, neutral charge, the dnp basis set, and a fine integration grid were employed. Symmetry was again activated, expected to benefit convergence for a molecule with the characteristics of TTF.

For B3LYP calculations, geometry optimization task parameters mirrored those of LDA-PWC and GGA-PBE, with key differences: symmetry was deactivated, allowing full unconstrained relaxation, and the functional was set to “b3lyp umesh=xcoarse minu=-3.” This denotes the use of a hybrid functional that combines exact exchange from Hartree–Fock theory with a modified mesh for coarse integration and a specified minimum potential value (minu) to improve numerical stability. As with the other methods, the electronic setup included spin-unrestricted polarization, zero net charge, the dnp basis set, no pseudopotentials, and a fine integration grid.

Following geometry optimization for each functional, further analyses were conducted. The electronic structure was examined by calculating the frontier molecular orbitals (FMOs), particularly the energies of the highest occupied molecular orbital (HOMO) and the lowest unoccupied molecular orbital (LUMO), from which the HOMO–

LUMO energy gap ( $\Delta E$ ) was determined. This gap serves as a key indicator of chemical reactivity, kinetic stability, and optical behavior [10][11].

Vibrational frequency calculations were performed using the harmonic oscillator approximation, enabling assignment of infrared (IR) spectra associated with distinct vibrational modes such as C–S bond stretching, C–H bending, and C=C stretching. The calculated frequencies and intensities were compared with experimental data, confirming the accuracy of the optimized geometries.

Comparative analysis of the three functionals revealed that LDA-PWC and GGA-PBE, both operating with symmetry enabled, offered computational efficiency and stable convergence. However, the hybrid B3LYP functional, despite its higher computational demands, yielded results more consistent with experimental observations regarding bond lengths, vibrational spectra, and electronic properties. This highlights the critical role of functional choice in DFT studies and supports the use of hybrid functionals for accurate modeling of conjugated organic systems such as TTF.

In summary, the present study integrates a structured DFT-based methodology encompassing geometry optimization, electronic structure evaluation, and vibrational analysis. The consistency of task parameters across LDA-PWC, GGA-PBE, and B3LYP—along with tailored adjustments for each functional—ensures a reliable and comparative assessment that facilitates a comprehensive understanding of the molecule's behavior and its potential applications in organic electronics.

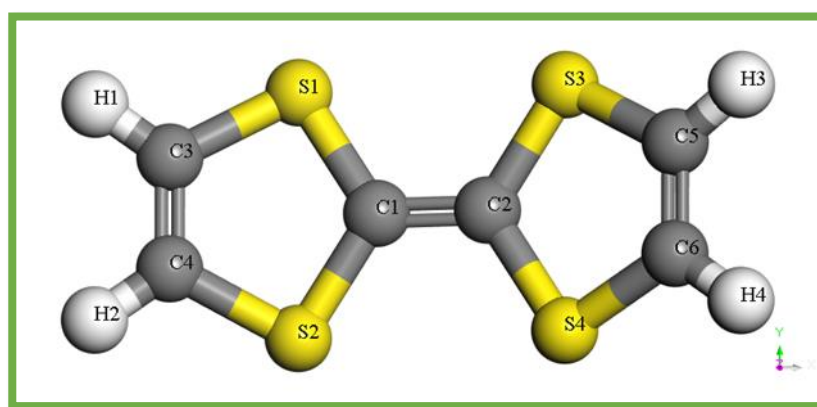


**Figure 2.** Optimized geometric structure of the TTF molecule.

### 3. Results and Discussion

#### 3.1 Optimized Parameters

##### 3.1.1 Optimized Bond Lengths

The optimized bond lengths of the TTF molecule were calculated using Density Functional Theory (DFT) with three different exchange–correlation functionals: LDA (Local Density Approximation), GGA (Generalized Gradient Approximation), and B3LYP (Becke, 3-parameter, Lee–Yang–Parr hybrid functional). Bond length is defined as the average distance between the nuclei of two chemically bonded atoms in a molecule and is typically measured in units such as angstroms (Å) or picometers (pm) [13]. Bond length depends on several factors, including the type of covalent bond—single, double, or triple—and is generally inversely proportional to bond order; higher bond orders result in shorter, stronger bonds [14].

The results show a clear functional dependence in the calculated bond lengths. The LDA functional tends to predict shorter bond lengths due to an overestimation of exchange energy and a simplified treatment of electron correlation [15][16]. In contrast, the GGA functional usually produces longer bond lengths by incorporating the gradient of electron density, thereby correcting some of the LDA's overbinding tendencies [15][17]. The B3LYP hybrid functional, which includes a portion of exact exchange from Hartree–Fock theory,

often achieves a balance, resulting in bond lengths that are typically more reliable for organic molecules [18].

Specifically, the C1–C2, C3–C4, and C5–C6 bonds were found to be shorter with LDA and longer with GGA, while B3LYP provided intermediate values. The C–S bond lengths exhibited a consistent trend of increasing in the order LDA < GGA < B3LYP. For the C–H bonds, B3LYP tended to predict slightly shorter lengths. The shortest observed bond lengths were 1.091 Å (LDA), 1.088 Å (GGA), and 1.079 Å (B3LYP), all associated with C–H bonds.

**Table 1.** Presents the optimized bond length values for the Tetrathiafulvalene (TTF) molecule calculated using Density Functional Theory (DFT) with the LDA, GGA, and B3LYP approximations, alongside a comparison with values reported in previous studies.

Parameter	Bond Lengths (Å)			
	LDA-PWC	GGA-PBE	B3YLB	Previous Work [19]
C1–C2	1.351	1.360	1.346	1.3468
C1–S1	1.752	1.778	1.787	1.7876
C1–S2	1.752	1.778	1.787	1.7876
C2–S3	1.752	1.778	1.788	1.7876
C2–S4	1.752	1.778	1.788	1.7876
C3–C4	1.338	1.344	1.331	1.3342
C3–H1	1.091	1.088	1.079	1.0812
C3–S1	1.74	1.758	1.761	1.76
C4–H2	1.091	1.088	1.080	1.0812
C4–S2	1.74	1.758	1.760	1.76
C5–C6	1.338	1.344	1.331	1.3342
C5–H3	1.091	1.088	1.080	1.0812
C5–S3	1.74	1.758	1.760	1.76
C6–H4	1.091	1.088	1.079	1.0812
C6–S4	1.74	1.758	1.761	1.76

### 3.1.2 Optimized Bond Angles

The bond angle values of the Tetrathiafulvalene (TTF) molecule were calculated using Density Functional Theory (DFT) with three different exchange-correlation functionals: LDA (Local Density Approximation), GGA (Generalized Gradient Approximation), and B3LYP (Becke, 3-parameter, Lee–Yang–Parr). A detailed analysis of the results reveals that the B3LYP method generally produces larger bond angles compared to LDA and GGA. While LDA and GGA yield relatively similar values, GGA tends to give slightly larger angles. Interestingly, the values predicted by B3LYP are often closer to previously reported results, indicating that it may provide a more accurate representation of the molecular geometry.

For example, bond angles such as A(C1, S1, C3) and A(C1, S2, C4) were predicted by LDA at 93.809°, by GGA at 94.165°, and by B3LYP at 94.883°, whereas previous data reported a value of 94.9765°. This suggests that the B3LYP method, which incorporates hybrid functionals to account for electronic interactions, yields values more consistent with reference results. Similarly, angles involving C2, C1, S1, and C2, C1, S2 increase gradually from LDA (122.747°) to GGA (122.986°) and then to B3LYP (123.228°) and (123.177°). Previous reference values (123.1184° and 123.1191°) closely match the B3LYP results, further validating their reliability. This increase in bond angles can be attributed to the improved treatment of electron exchange and correlation effects by the B3LYP method [18].



**Table 2.** Optimized bond angle values of the TTF molecule calculated using DFT with LDA, GGA, and B3LYP approximations, along with a comparison to values reported in previous studies.

Parameter	Bond Angle (°)			
	LDA-PWC	GGA-PBE	B3YLB	Previous Work [19]
A(C1,S1,C3)	93.809	94.165	94.883	94.9765
A(C1,S2,C4)	93.809	94.165	95.09	94.9763
A(C2,C1,S1)	122.747	122.986	123.228	123.1184
A(C2,C1,S2)	122.747	122.986	123.177	123.1191
A(C2,S3,C5)	93.809	94.165	95.08	94.9763
A(C2,S4,C6)	93.809	94.165	94.887	94.9765
A(C3,C4,H2)	125.012	125.004	125.134	124.838
A(C5,C6,H4)	125.012	125.004	124.821	124.838
A(C6,C5,H3)	125.012	125.004	125.144	124.838
A(C6,C5,S3)	117.534	117.773	117.962	118.1423
A(S1,C1,S2)	114.494	114.025	113.592	113.7625
A(S1,C3,H1)	117.366	117.159	116.876	117.0196
A(S1,C3,C4)	117.534	117.773	118.309	118.1424
A(S2,C4,C3)	117.534	117.773	119.967	118.1423
A(S2,C4,H2)	117.366	117.159	116.89	117.0197
A(S3,C2,C1)	122.747	122.986	123.233	123.1191
A(C4,C3,H1)	125.012	125.004	124.815	124.838
A(S3,C5,H3)	117.366	117.159	116.885	117.0197
A(S4,C2,C1)	122.747	122.986	123.186	123.1184
A(S4,C2,S3)	114.494	114.025	113.579	113.7625
A(S4,C6,C5)	117.534	117.773	118.289	118.1424
A(S4,C6,H4)	117.366	117.159	116.889	117.0196

### 3.2 Frontier Molecular Orbitals (FMOs)

Frontier Molecular Orbitals (FMOs)—specifically the Highest Occupied Molecular Orbital (HOMO) and the Lowest Unoccupied Molecular Orbital (LUMO)—play a pivotal role in understanding chemical reactivity, electronic properties, and molecular interactions. These orbitals represent the boundary between the occupied and unoccupied molecular orbitals in the electronic configuration of a molecule. The HOMO is the highest energy orbital containing electrons, whereas the LUMO is the lowest energy orbital without electrons. These orbitals determine how the molecule interacts with its environment, making them essential for predicting reactivity, stability, and optical behavior [10][20].

According to Frontier Molecular Orbital theory, chemical reactions are dominated by the interaction between the HOMO of one molecule and the LUMO of another. A molecule with a high-energy HOMO generally acts as an electron donor, while a molecule with a low-energy LUMO serves as a good electron acceptor. The energy gap between HOMO and LUMO, denoted as  $\Delta E$ , serves as an indicator of the chemical stability and kinetic reactivity of the molecule; a smaller gap typically correlates with higher reactivity and lower stability [11]. This energy gap is also used to explain electronic and optical properties in conjugated systems and semiconductors [18].

The data in Table (3) reveal significant variations depending on the functional employed. The LDA-PWC and GGA-PBE functionals predict higher HOMO energies (-4.124 eV and -3.996 eV, respectively) compared to B3LYP (-4.562 eV) and reference values (-4.734 eV), suggesting a possible overestimation of the ionization potential of the TTF molecule. Conversely, LDA-PWC and GGA-PBE yield lower LUMO energies (-1.991 eV

and -1.892 eV, respectively) relative to B3LYP (-1.114 eV) and previous results (-1.193 eV), which may indicate an overestimation of electron affinity.

More importantly, LDA-PWC and GGA-PBE significantly underestimate the HOMO-LUMO energy gap (2.133 eV and 2.104 eV, respectively) compared to B3LYP (3.448 eV) and the reference value (3.541 eV). Since the energy gap correlates with molecular reactivity and conductivity, the choice of functional strongly influences the accuracy of predicting these properties. These results indicate that despite the computational efficiency of LDA-PWC and GGA-PBE, they may not be suitable for precise electronic structure calculations of the TTF molecule. In contrast, B3LYP, as a hybrid functional, provides results closer to reference data, highlighting its superior performance in this context. Therefore, when using DFT to study TTF or similar systems, careful selection of the functional is essential to ensure reliable results.

**Table 3.** HOMO, LUMO energy values and the energy gap ( $\Delta E$ ) calculated using LDA-PWC, GGA-PBE, and B3LYP functionals.

Molecular Orbital	LDA-PWC	GGA-PBE	B3LYP	Previous Work [19]
HOMO Energy (Ev)	-4.124	-3.996	-4.562	-4.734
LUMO Energy (Ev)	-1.991	-1.892	-1.114	-1.193
Energy Gap (Ev)	2.133	2.104	3.448	3.541

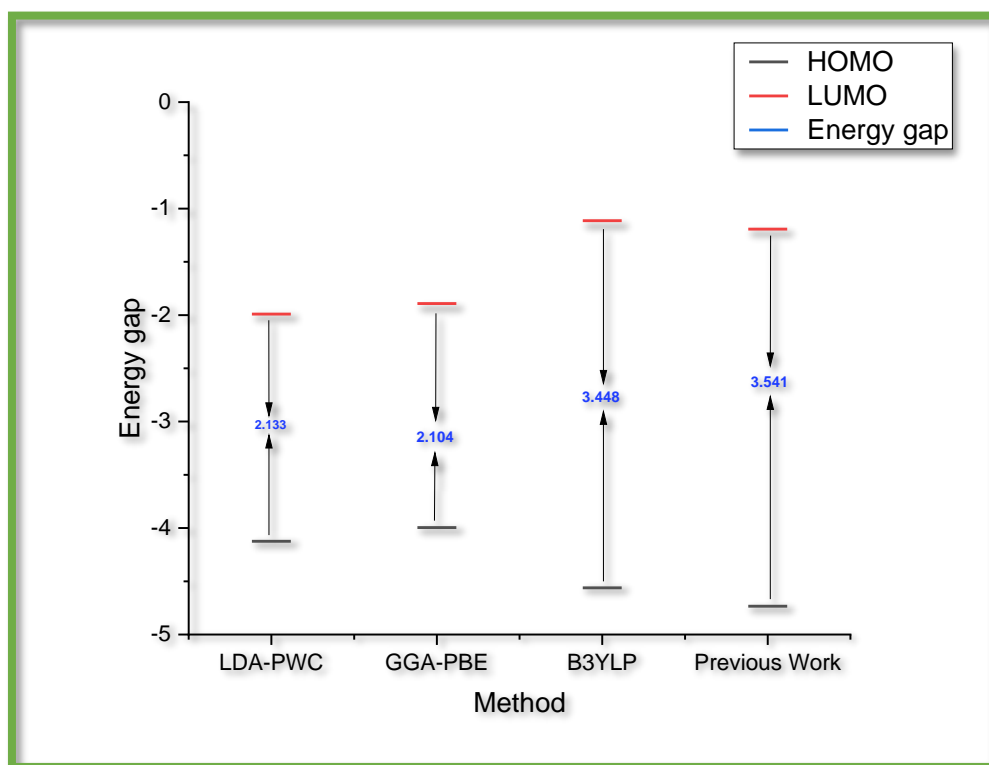


**Figure 3.** A graphical plot illustrating the HOMO and LUMO energy values as well as the energy gap ( $\Delta E$ ) calculated using the LDA-PWC, GGA-PBE, and B3LYP functionals.

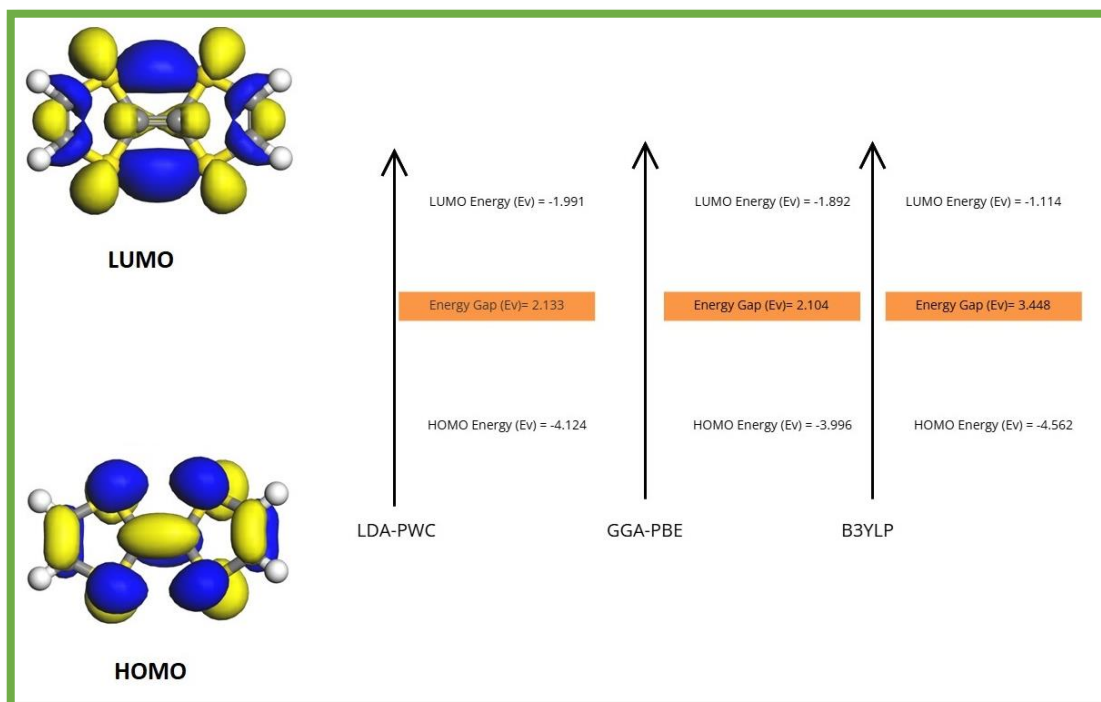


**Figure 4.** A schematic diagram of the HOMO and LUMO molecular orbitals of the TTF molecule.

### 3.3 Global Chemical Reactivity Descriptors (GCRDs)

Global Chemical Reactivity Descriptors (GCRDs) are important quantitative tools for understanding the electronic structure and chemical behavior of molecules. These descriptors are derived from the energies of the frontier molecular orbitals and include: Ionization Potential (IP), Electron Affinity (EA), Chemical Hardness ( $\eta$ ), Softness (S), Chemical Potential ( $\mu$ ), Electronegativity ( $\chi$ ), and Electrophilicity Index ( $\omega$ ). These indicators provide an effective means in theoretical chemistry to predict molecular reactivity, stability, and selectivity. Understanding molecular reactivity and stability is fundamental in fields such as organic synthesis, drug design, and materials science. Within the framework of Density Functional Theory (DFT), GCRDs have emerged as a powerful quantitative framework for analyzing reactive patterns of molecules, linking their electronic structure to chemical behavior. They are particularly useful when experimental data are scarce or unavailable [10].

The theoretical formulation of global reactivity descriptors is based on Koopmans' theorem, which approximates the ionization potential (IP) and electron affinity (EA) as the negative of the HOMO and LUMO energies, respectively [21]. Based on these orbital energies, the following descriptors are defined:

$$(IP) = -E(\text{HOMO}), (EA) = -E(\text{LUMO}), (\eta) = (IP - EA)/2, (\mu) = -(IP + EA)/2$$

$$(\chi) = -\mu = (IP + EA)/2, (S) = 1/\eta, (\omega) = \mu^2/2\eta$$

These descriptors were developed within the DFT framework by Parr and Pearson [22], providing a consistent method for analyzing molecular reactivity. Chemical hardness and softness reflect a molecule's resistance or readiness to change its electronic distribution, while chemical potential and electronegativity indicate the tendency to lose or gain electrons. The electrophilicity index, introduced by Parr and co-workers [23], measures the energy stabilization when the molecule acquires an additional electronic charge.

These descriptors were calculated using quantum chemical methods based on DFT and approximate functionals such as LDA, GGA, and hybrid functionals like B3LYP to compute orbital energies. Although Koopmans' theorem is an approximation within DFT,



the general trends provided by GCRDs often correlate well with experimental observations [24].

Table (4) presents the HOMO and LUMO energies, and consequently the derived IP and EA values for TTF, calculated using different DFT functionals: LDA-PWC, GGA-PBE, and B3LYP, along with data from previous work for comparison. From these values, the approximate IP and EA of TTF can be estimated using Koopmans' approximations: for LDA-PWC, IP  $\approx$  4.124 eV and EA  $\approx$  1.991 eV; for GGA-PBE, IP  $\approx$  3.996 eV and EA  $\approx$  1.892 eV; and for B3LYP, IP  $\approx$  4.562 eV and EA  $\approx$  1.114 eV. A clear functional dependence is observed: LDA-PWC and GGA-PBE predict lower IP and higher EA values compared to B3LYP and previous studies, indicating a tendency to overestimate the ease of both oxidation and reduction of TTF relative to B3LYP and the reference data. The B3LYP functional yields values closer to the previous work for both IP and EA, suggesting that within this dataset, B3LYP provides a more accurate representation of the electronic properties of TTF.

**Table 4.** Shows the values of ionization potential (IP) and electron affinity (EA) derived from the HOMO and LUMO energies.

Method	HOMO	LUMO	IP (Ev)	EA (eV)
LDA-PWC	-4.124	-1.991	4.124	1.991
GGA-PBE	-3.996	-1.892	3.996	1.892
B3LYP	-4.562	-1.114	4.562	1.114
Previous Work (25)	4.7345	-1.1927	4.7345	1.1927

Regarding the other chemical reactivity descriptors, Table (5) presents these values. Chemical hardness ( $\eta$ ), which indicates resistance to changes in the electronic structure, is lower for LDA-PWC (1.0665) and GGA-PBE (1.052) compared to B3LYP (1.724) and previous work (1.770), suggesting a potential underestimation of TTF's stability by the former functionals. Conversely, softness ( $S$ ), describing polarizability, is higher for LDA-PWC (0.9376) and GGA-PBE (0.9506) relative to B3LYP (0.5799) and previous data (0.564).

The chemical potential ( $\mu$ ), reflecting the tendency to lose electrons, is slightly lower for LDA-PWC (-3.0575) and GGA-PBE (-2.944) than for B3LYP (-2.838) and previous work (-2.963), indicating a slight overestimation of TTF's electron-donating ability. The electrophilicity index ( $\omega$ ), which measures electron affinity, is significantly higher for LDA-PWC (4.389) and GGA-PBE (4.115) compared to B3LYP (2.338) and earlier studies (2.479), suggesting an exaggeration of TTF's electrophilic nature.

The choice of DFT functional thus strongly influences the computed electronic properties of TTF. LDA-PWC and GGA-PBE tend to predict lower chemical hardness and higher electrophilicity values than B3LYP and previous reports. In contrast, B3LYP results closely match prior work across all descriptors. These discrepancies highlight the importance of selecting an appropriate functional to achieve accurate molecular property predictions, especially for organic molecules such as TTF.

**Table 5.** shows the values of the chemical reactivity descriptors for the TTF molecule calculated using DFT with the LDA-PWC, GGA-PBE, and B3LYP functionals.

Parameters	LDA-PWC	GGA-PBE	B3LYP	Previous Work (19)	Unit
Chemical Hardness ( $\eta$ )	1.0665	1.052	1.724	1.770	eV
Chemical Softness ( $S$ )	0.9376	0.9506	0.5799	0.564	1/eV
Chemical Potential ( $\mu$ )	-3.0575	-2.944	-2.838	-2.963	eV
Electronegativity ( $\chi$ )	3.0575	2.944	2.838	2.963	eV
Electrophilicity Index ( $\omega$ )	4.389	4.115	2.338	2.479	eV

### 3.4 Vibrational Frequencies and IR Intensities

The study of vibrational frequencies constitutes a fundamental application in quantum chemistry, providing a vital link between theoretical calculations and experimental spectroscopic analysis. This approach enables the identification of molecular vibrational modes, the estimation of thermodynamic properties, and the confirmation of structural stability through the absence of imaginary frequencies. When combined with the calculation of infrared (IR) intensities, this methodology becomes a powerful tool for interpreting and assigning spectral signals [24].

In this context, tetrathiafulvalene (TTF) attracts particular interest as a prototypical system in organic electronics and charge-transfer compounds due to its high electron-donating capabilities. Understanding its vibrational behavior is crucial for characterizing its structure, reactivity, and solid-state interactions [5]. In quantum chemistry, vibrational frequencies are computed from the second derivatives of the total molecular energy with respect to nuclear displacements, forming the Hessian matrix. Vibrational modes and their associated frequencies are obtained through mass-weighted diagonalization of this matrix. Under the harmonic approximation, molecules are assumed to undergo small displacements around their equilibrium geometries, with the potential energy surface approximated as a quadratic function [12].

The vibrational frequencies and IR intensities of the TTF molecule were calculated using DFT methods with different exchange-correlation functionals, including LDA-PWC, GGA-PBE, and B3LYP. All computations were performed using the Dmol<sup>3</sup> software package, where the molecular geometry was first optimized, followed by frequency calculations using analytical second derivatives of the energy.

The computed IR intensities exhibit prominent peaks near 600 cm<sup>-1</sup>, 800 cm<sup>-1</sup>, and 1600 cm<sup>-1</sup>, indicating significant vibrational activity in these regions, as illustrated in Figures 5, 6, and 7.

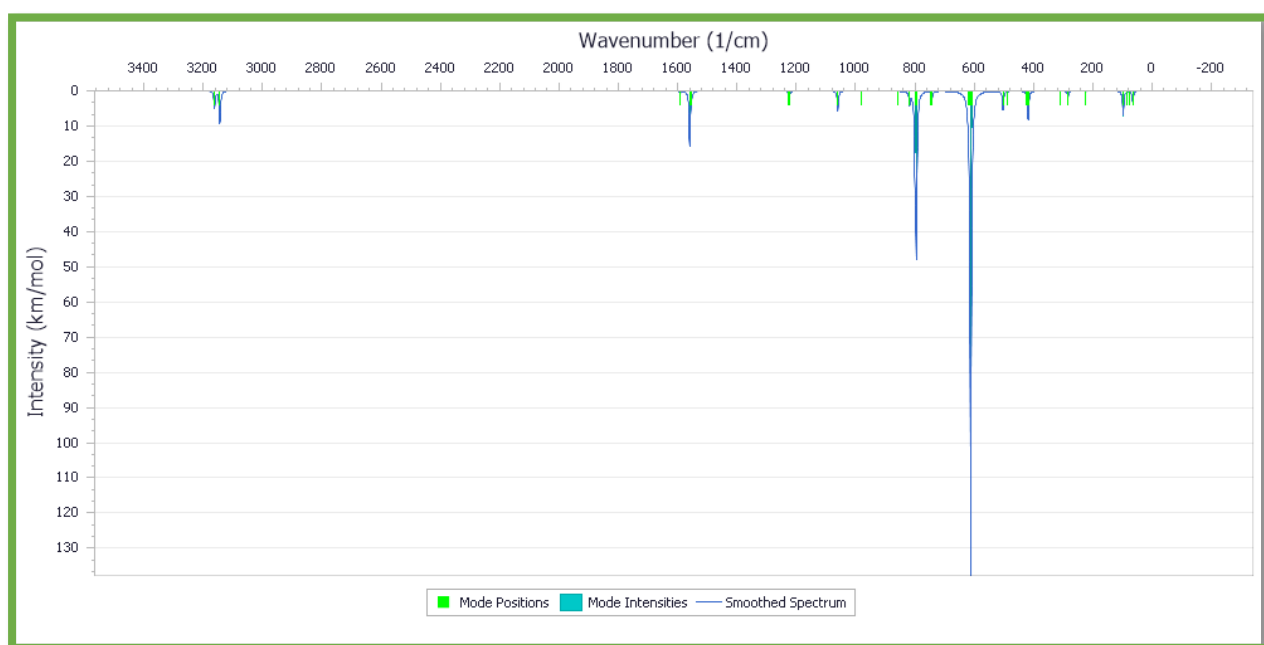


**Figure 5.** shows the infrared (IR) intensities and vibrational frequencies of the TTF molecule calculated using DFT with the LDA-PWC approximation.



**Figure 6.** shows the infrared (IR) intensities and vibrational frequencies of the TTF molecule calculated using DFT with the GGA-PBE approximation.

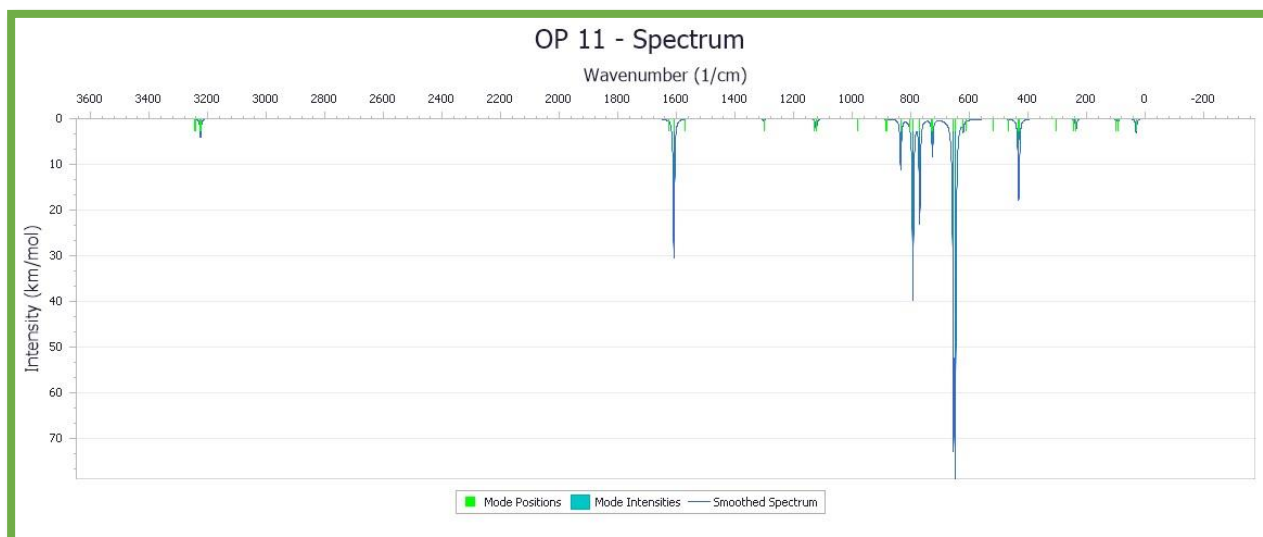


**Figure 7.** shows the infrared (IR) intensities and vibrational frequencies of the TTF molecule calculated using DFT with the B3LYP approximation.

In the low-frequency region ( $0\text{--}1000\text{ cm}^{-1}$ ), the peaks around  $600\text{ cm}^{-1}$  are likely associated with the stretching and bending vibrations of the C–S bonds. These vibrations contribute significantly to the structural flexibility of the TTF molecule, thereby influencing its overall stability. The prominent peak near  $600\text{ cm}^{-1}$ , attributed to C–S stretching modes, indicates strong bonding interactions involving sulfur atoms, which are critical to the conductive properties of TTF.

Within the mid-frequency range ( $1000\text{--}1600\text{ cm}^{-1}$ ), the notable peak around  $1600\text{ cm}^{-1}$  with strong intensity corresponds to bending vibrations of the C–H bonds, enhancing understanding of hydrogen atom interactions within the molecule, as well as C=C bond stretching vibrations, which are essential for TTF's behavior as an electron donor [26]. This fundamental peak at  $1600\text{ cm}^{-1}$ , characterized by high intensity, reflects significant dipole moment changes [27], making this vibrational mode highly active in the infrared spectrum.

In the high-frequency region ( $1600\text{--}3200\text{ cm}^{-1}$ ), the main peak around  $3100\text{ cm}^{-1}$  is assigned to C–H stretching vibrations in the Tetrathiafulvalene (TTF) molecule, indicating the presence of C–H bonds in an unsaturated chemical environment within a conjugated

electronic system. This distinguishes these vibrations from those of C–H bonds in alkanes, which typically occur between 2850 and 2960  $\text{cm}^{-1}$  [31].

Comparative analysis of the three computational methods—LDA-PWC, GGA-PBE, and B3LYP—reveals consistent trends in vibrational frequencies, with peaks appearing in similar regions. Minor variations in peak positions and intensities reflect methodological differences inherent to each theoretical approach [28]. Table (6) presents a comparison of the vibrational frequencies and IR intensities obtained by the three methods alongside previous experimental and theoretical studies, showing generally consistent data with slight discrepancies attributable to methodological variances.

**Table 6.** shows the vibrational frequencies and infrared intensities calculated using the Density Functional Theory (DFT) method with the LDA-PWC, GGA-PBE, and B3LYP approximations, compared to data obtained from previous experimental studies.

Vibrational Frequencies and IR Intensities of TTF								
Mode	LDA-PWC		GGA-PBE		B3LYP		Previous Work [19]	
	Frequency (1/cm)	Intensity (km/mol)	Frequency (1/cm)	Intensity (km/mol)	Frequency (1/cm)	Intensity (km/mol)	Frequency (1/cm)	Intensity (km/mol)
1	65.31	3.12	36.96	1.8	31.12	2.98	28.2373	3.7866
2	75.51	0	76.67	0	91.69	0.01	76.5584	0.0002
3	85.44	0.37	80.61	4.22	92.76	0.52	81.0886	0
4	97.68	7.07	106.25	0.35	98.45	0.28	107.6761	0.5729
5	223.97	0.19	228.24	0.61	236.36	2.36	237.5959	0.8796
6	283.34	1.98	267.15	1.85	245.14	0	250.26	0.0001
7	308.37	0	303.06	0	304.16	0	305.013	0
8	417.77	8.3	409.11	0	429.66	4.43	407.6907	0
9	421.85	0	412.54	0	432.42	15.66	414.8	0
10	425.88	0.01	417.97	8.66	433.54	0.03	435.0598	20.3545
11	488.01	0	477.09	0.13	466.71	0	468.3674	0
12	502.98	5.53	479.18	7.27	517.66	0	512.4114	0.0002
13	609.11	10.51	605.71	0	612.87	0	614.8623	0
14	611.84	137.68	611.81	1.39	621.3	2.08	624.7912	2.0915
15	616.35	0	689.94	5.06	648.4	69.77	641.0365	0.0001
16	621.09	0.78	692.5	130.06	654.59	62.7	643.2925	131.6045
17	742.1	1.98	729.71	4.88	726.43	8.12	729.7315	12.178
18	747.55	0.06	733.4	1.49	728.95	0	732.405	0
19	794.9	44.68	779.39	18.21	769.95	22.53	768.9768	26.1163
20	799.68	17.5	794.26	44.76	793.09	39.31	791.5905	55.4767
21	800.26	0	799.87	0	805.31	0.03	800.5423	0
22	817.39	3.36	829.23	0.45	834.86	10.92	830.4742	6.181
23	818.07	0	878.67	0	881.09	0.17	862.2408	0
24	858.82	0	878.86	0.61	885.14	0.05	863.2276	0
25	979.96	0	961.26	0	981.7	0	972.6813	0
26	1059.69	4.97	1110.63	3.93	1123.26	2.66	1121.6268	2.5574
27	1060.63	1.22	1111.27	0.62	1128.34	0.05	1122.0201	0
28	1224.26	1.94	1274.67	1.19	1299.5	0.04	1284.1174	0.0019
29	1228.02	0	1277.26	0	1302.11	0.48	1286.4421	0
30	1553.4	0.75	1497.1	0.29	1572.77	0	1574.7862	0
31	1559.31	15.73	1514.38	22.28	1609.16	30.49	1594.7101	42.344
32	1591.25	0.6	1536.64	0.68	1626.14	0	1619.9591	0
33	3144.05	0	3157.31	0	3223.7	0.02	3206.8385	0

34	3144.18	9.37	3157.44	3.58	3225.12	4.05	3207.0669	5.8909
35	3162.07	4.52	3175.39	0.01	3242.8	0.2	3226.8519	0.0222
36	3162.12	0.34	3175.44	0	3244.21	0	3226.9335	0

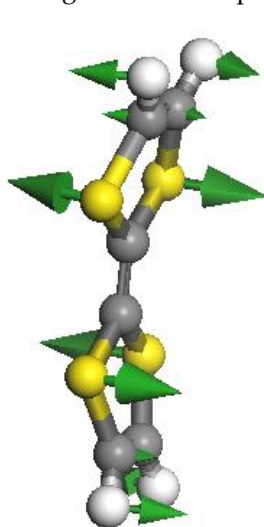
Understanding these vibrational frequencies and infrared intensities is crucial for applications in organic electronics and conductive materials. The strong C=C stretching mode observed near  $\sim 1600\text{ cm}^{-1}$  supports the role of tetrathiafulvalene (TTF) as an organic donor molecule. Additionally, the structural vibrations in the low-frequency region provide insights into the rigidity and flexibility of the molecule, which are essential for charge transport properties. Further computational and experimental studies can offer deeper understanding of the vibrational behavior and electronic interactions of the TTF molecule, thereby enhancing its applications in advanced materials and technologies [29].

### 3.5 Vibration Modes

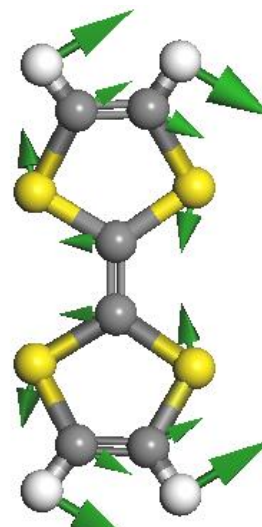
Knowledge of molecular vibrational modes provides valuable information about the molecular structure, properties, interactions, and applications across various fields [30]. Vibrational analysis is a powerful tool in scientific research and technological applications. In this study, a detailed computational analysis of the vibrational modes of the tetrathiafulvalene (TTF) molecule is presented. TTF is well-known for its conjugated structure and redox properties, making it particularly significant in the field of organic electronics. The vibrational frequencies, intensities, and symmetry assignments obtained through quantum chemical calculations using Density Functional Theory (DFT) with LDA-PWC, GGA-PBE, and B3LYP approximations, implemented via the Dmol3 software, are employed to elucidate the intrinsic molecular dynamics and their potential impact on the electronic behavior of the TTF molecule.

Initially, the full geometric optimization of the TTF molecule was performed to ensure that the structure corresponds to a true stable minimum, confirmed by the absence of imaginary (negative) frequencies. For this nonlinear molecule, consisting of approximately 14 atoms with the formula ( $\text{C}_6\text{H}_4\text{S}_4$ ), 36 vibrational modes are expected according to the formula ( $3N-6$ ).

The analysis of frequency ranges and mode assignments in the vibrational spectrum is a fundamental aspect of understanding molecular motions. The spectrum was divided into several regions, each corresponding to specific types of molecular motions. In the low-frequency region (below  $1000\text{ cm}^{-1}$ ), the vibrations typically involve C-S bending modes and various ring deformation patterns.



Mode 2: Approximately  $76.67\text{ cm}^{-1}$

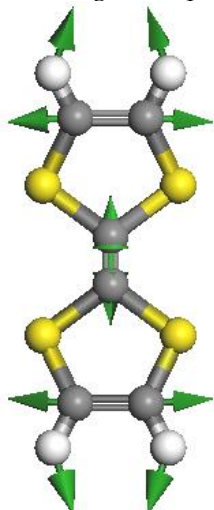


Mode 4: Approximately  $106.25\text{ cm}^{-1}$

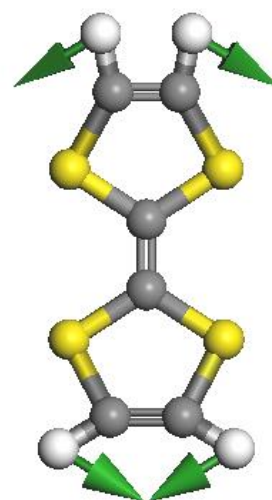
The mid-frequency region ( $1000\text{--}1600\text{ cm}^{-1}$ ) encompasses C=C stretching modes and C-H bending modes, with precise positions depending on the specific mode and coupling



with other vibrations. These modes are essential for understanding the electronic properties and charge transport capabilities of TTF.

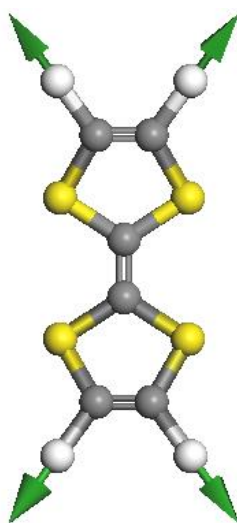


Mode 32: Approximately  $1536.64\text{ cm}^{-1}$

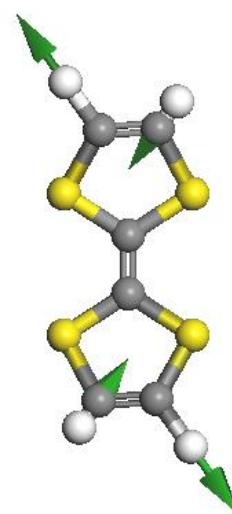


Mode 26: Approximately  $1110.63\text{ cm}^{-1}$

In the high-frequency range of  $3000\text{ cm}^{-1}$  and above, C–H stretching vibrations are observed. This frequency serves as an indicator of relatively linear and  $\pi$ -conjugated C–H bonds, reflecting the molecular structure's rigidity and stability [5]. These structural characteristics enhance the molecule's ability to function as an organic conductor by facilitating smooth electron transport across the molecular surface.



Mode 36: Approximately  $3175.44\text{ cm}^{-1}$



Mode 33: Approximately  $3157.31\text{ cm}^{-1}$

In this manner, the analysis of frequency ranges and mode assignments forms a comprehensive framework for understanding molecular motions in the vibrational spectrum. This approach enables the interpretation of molecular behavior under various conditions and contributes to the advancement of its applications in fields such as organic electronics.

#### 4. Conclusion

This study presented a detailed quantum analysis of the structural, electronic, vibrational, and thermodynamic properties of the tetrathiafulvalene (TTF) molecule, a sulfur-rich organic compound, with the aim of evaluating its semiconducting capabilities through Density Functional Theory (DFT) calculations. The comparative assessment between the LDA-PWC, GGA-PBE, and B3LYP functionals provided deep insights into

how theoretical modeling influences the interpretation of TTF's unique electronic and physical behavior.

The results demonstrated that the TTF molecule possesses structural features favorable for  $\pi$ -conjugation and electronic coupling, supported by its planar configuration and the presence of sulfur atoms. Notably, the hybrid B3LYP functional exhibited superior accuracy in describing bond lengths and angles, underpinning the formation of a stable electronic structure—an essential factor in organic conductivity.

The analysis of frontier molecular orbitals revealed an energy gap between the HOMO and LUMO levels of approximately 3.45 eV (according to B3LYP), consistent with moderate semiconductor behavior. Additionally, the elevated HOMO level and low ionization potential indicate TTF's strong electron-donating ability, a key characteristic of p-type organic semiconductors. The sulfur atoms contribute to enhancing electronic polarization and coupling through S...S interactions and  $\pi$ - $\pi$  stacking, thereby improving charge transfer efficiency between molecules.

Vibrational spectra confirmed the stability of the molecular structure and identified major modes associated with C-S and C=C bond vibrations, which are critical for molecular flexibility and charge transport, particularly in the solid state and charge-transfer complexes.

Thermodynamic analyses revealed TTF's good thermal adaptability, with heat capacity and enthalpy increasing steadily with temperature, while free energy decreases following the expected Gibbs equation behavior. This indicates favorable thermal stability, a crucial requirement for organic materials operating under varied thermal conditions.

Overall, the theoretical data confirm that TTF embodies fundamental attributes as a sulfur-containing organic semiconductor. Its electronic properties, vibrational stability, and thermodynamic behavior support its effectiveness as a molecular electronic component, especially in charge-transfer salts, organic conductors, and advanced optoelectronic devices. These findings also emphasize the importance of selecting an appropriate functional in DFT calculations to ensure accurate characterization of efficient organic materials.

## REFERENCES

- [1] K. Boubekur and P. Batail, "Tetrathiafulvalene (TTF) and its derivatives: fundamental aspects and applications," *Chemical Reviews*, vol. 100, no. 4, pp. 1025–1074, 2000.
- [2] E. M. Pérez and N. Martín, "Tetrathiafulvalene-based molecular systems: toward better conductors, switches, and sensors," *Chemical Society Reviews*, vol. 35, no. 6, pp. 593–607, 2006.
- [3] C. K. Chiang *et al.*, "Electrical conductivity in doped polyacetylene," *Physical Review Letters*, vol. 39, p. 1098, 1977.
- [4] F. Wudl, G. M. Smith, and E. J. Hufnagel, "Electrically Conducting Organic Materials. II. Tetrathiofulvalene, a Novel Electron Donor," *Journal of the American Chemical Society*, vol. 92, no. 2, pp. 589–590, 1970.
- [5] R. Kato, "Conducting molecular crystals based on TTF derivatives," *Chemical Reviews*, vol. 104, no. 11, pp. 5319–5346, 2004.
- [6] A. Facchetti, "Semiconductors for organic transistors," *Materials Today*, vol. 10, no. 3, pp. 28–37, 2007.
- [7] C. Ravikumar, J. I. Hubert, and D. Sajan, "Vibrational Contributions to the Second-Order Nonlinear Optical Properties of  $\pi$ -Conjugated Structure Acetoacetanilide," *Journal of Chemical Physics*, vol. 369, pp. 1–7, 2010.
- [8] B. A. Saleha, "Structure and vibrational spectra of mononitrated benzo[a]pyrenes," *Journal of Molecular Structure*, vol. 915, p. 47, 2009.
- [9] B. Delley, "From molecules to solids with the DMol<sup>3</sup> approach," *The Journal of Chemical Physics*, vol. 113, no. 18, pp. 7756–7764, 2000.
- [10] R. G. Parr and W. Yang, *Density-Functional Theory of Atoms and Molecules*. Oxford: Oxford University Press, 1989.

- [11] R. G. Pearson, "Absolute electronegativity and hardness: Application to inorganic chemistry," *Inorganic Chemistry*, vol. 27, no. 4, pp. 734–740, 1986.
- [12] D. A. McQuarrie and J. D. Simon, *Physical Chemistry: A Molecular Approach*. University Science Books, 1997.
- [13] P. Atkins and J. de Paula, *Physical Chemistry*, 9th ed. Oxford: Oxford University Press, 2010.
- [14] T. L. Brown, H. E. LeMay, B. E. Bursten, C. Murphy, and P. Woodward, *Chemistry: The Central Science*, 14th ed. Pearson, 2018.
- [15] J. P. Perdew and A. Zunger, "Self-interaction correction to density-functional approximations for many-electron systems," *Physical Review B*, vol. 23, no. 10, pp. 5048–5079, 1981.
- [16] R. M. Martin, *Electronic Structure: Basic Theory and Practical Methods*. Cambridge: Cambridge University Press, 2004.
- [17] G. Kresse and J. Furthmüller, "Efficiency of ab-initio total energy calculations for metals and semiconductors using a plane-wave basis set," *Computational Materials Science*, vol. 6, no. 1, pp. 15–50, 1996.
- [18] A. D. Becke, "Density-functional thermochemistry. III. The role of exact exchange," *The Journal of Chemical Physics*, vol. 98, no. 7, pp. 5648–5652, 1993.
- [19] L. S. Taura, R. Muhammad, A. Lawal, and A. S. Gidado, "Electronic structure and IR spectra analysis of tetrathiafulvalene (TTF) using RHF and DFT quantum mechanical methods," *Journal of Energy Research and Reviews*, vol. 10, pp. 20–35, 2022.
- [20] K. Fukui, "A molecular theory of reactivity in aromatic hydrocarbons," *The Journal of Chemical Physics*, vol. 20, no. 4, pp. 722–725, 1952.
- [21] T. Koopmans, "Über die Zuordnung von Wellenfunktionen und Eigenwerten zu den einzelnen Elektronen eines Atoms," *Physica*, vol. 1, no. 1–6, pp. 104–113, 1934.
- [22] R. G. Parr and R. G. Pearson, "Absolute hardness: companion parameter to absolute electronegativity," *Journal of the American Chemical Society*, vol. 105, no. 26, pp. 7512–7516, 1983.
- [23] R. G. Parr, L. V. Szentpály, and S. Liu, "Electrophilicity index," *Journal of the American Chemical Society*, vol. 121, no. 9, pp. 1922–1924, 1999.
- [24] F. Jensen, *Introduction to Computational Chemistry*, 3rd ed. Wiley, 2017.
- [25] R. N. Muhammad, N. M. Mahraz, A. S. Gidado, and A. Musa, "Theoretical study of solvent effects on the electronic and thermodynamic properties of tetrathiafulvalene (TTF) molecule based on DFT," *Asian Journal of Research and Reviews in Physics*, vol. 5, no. 2, 2021.
- [26] T. Shimanouchi, "Tables of Molecular Vibrational Frequencies Part 5," *Journal of Physical and Chemical Reference Data*, vol. 1, pp. 189, 1972.
- [27] N. A. Hasim, S. A. Aljunid, N. A. M. Ahmad Hambali, C. B. M. Rashidi, and R. Endut, "Identification of C-H bond vibration mode using absorption spectroscopy by a simple optically configured setup," *Jurnal Optoelektronik*, 2021.
- [28] D. S. Sholl and J. A. Steckel, *Density Functional Theory: A Practical Introduction*. Wiley, 2009.
- [29] A. Łapiński, "Vibrational and electronic structure, electron-electron and electron-phonon interactions in organic conductors investigated by optical spectroscopy," *IntechOpen*, 2016.
- [30] J. M. Hollas, *Modern Spectroscopy*, 4th ed. Wiley, 2004.
- [31] R. M. Silverstein, F. X. Webster, D. J. Kiemle, and D. L. Bryce, *Spectrometric Identification of Organic Compounds*, 8th ed. Wiley, 2014.